ACSNANO

www.acsnano.org

ARTICLE

Demystifying Trion Emission in CdSe Nanoplatelets

Maurizio Riesner, Farzan Shabani, Levin Zeylmans van Emmichoven, Julian Klein, Savas Delikanli, Rachel Fainblat, Hilmi Volkan Demir, and Gerd Bacher*

Cite This: *ACS Nano* 2024, 18, 24523−24531

Read Online

ACCESS | Metrics & More | Article Recommendations | Supporting Information

ABSTRACT: At cryogenic temperatures, the photoluminescence spectrum of CdSe nanoplatelets (NPLs) usually consists of multiple emission lines, the origin of which is still under debate. While there seems to be consensus that both neutral excitons and trions contribute to the NPL emission, the prominent role of trions is rather puzzling. In this work, we demonstrate that Förster resonant energy transfer in stacks of NPLs combined with hole trap states in specific NPLs within the stack trigger trion formation, while single NPL spectra are dominated by neutral excitonic emission. This interpretation is verified by implementing copper (Cu^+) dopants into the lattice as intentional hole traps. Trion emission gets strongly enhanced, and due to the large amount of hole trapping Cu^+ states in each single NPL, trion formation does not necessarily require stacking of NPLs. Thus, the ratio between trion and neutral exciton emission can be controlled by either changing the amount of stacked NPLs during sample preparation or implementing copper dopants into the lattice which act as additional hole traps.

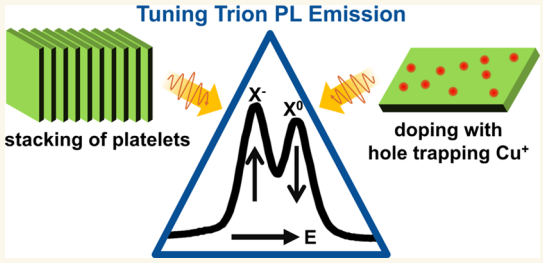

KEYWORDS: *CdSe nanoplatelets, photoluminescence, trion, exciton, copper doping, single nanoplatelet spectroscopy, FRET*

Quasi two-dimensional colloidal semiconductor nanoplatelets (NPLs, also known as colloidal quantum wells (CQWs)) can be synthesized with a precise thickness of only a few atomic layers leading to a strong vertical quantum confinement.[1,2] CdSe-based NPLs show excellent electronic and optical properties, such as ultra narrow absorption and emission lines,[3] high quantum yield,[4] giant oscillator strength[5] and ultralow threshold lasing[6] and have been proven themselves as excellent candidates for numerous applications, including lasers,[7] light emitting diodes,[8] photodetectors[9] and phototransistors.[10] Doping the NPLs adds an additional degree of freedom for tuning their optoelectronic properties and extending the range of applications. Among the several successfully implemented transition metal dopants into CdSe NPLs, copper doping results in midgap states, which lead to a long lifetime Stokes-shifted emission,[11−14] essential for applications including, *e.g.*, luminescent solar concentrators with near-unity efficiency[15] and photocatalysts.[16]

Due to their large oscillator strength, their monodispersity, and their ability to stack densely, NPLs have proven themselves as a platform for an ultraefficient Förster resonant energy transfer (FRET), a nonradiative dipole−dipole interaction between donors and acceptors.[17] In a stack of NPLs an exciton in a certain NPL recombines and transfers its energy nonradiatively to a neighboring NPL (funneling). Hereby, the transfer efficiency is determined by the spectral overlap of emission and absorption of the two NPLs and their distance. If donors and acceptors are from different species (e.g., NPLs consisting of a different number of monolayers) the energy transfer is called hetero-FRET, which can be directly accessed.[18] In case donor and acceptor are from the same species (e.g., NPLs with the same number of monolayers, homo-FRET), the overlap of emission and absorption from the donor and the acceptor, respectively, is significantly enhanced, i.e. the Stokes shift is very small. This drastically increases the FRET efficiency, which can lead to an exciton transfer via FRET of up to 500 nm within a stack before the excitons are recombining radiatively.[19] This exciton diffusion through a stack of NPLs has been argued to lead to a quenching of the photoluminescence (PL)[20,21] or even to a collective blinking of a single stack of NPLs.[22]

It has been shown that at temperatures below 100 K the PL spectrum of CdSe NPLs consists of two or even three well separated emission lines.[23−25] One line is usually attributed to

Received: July 1, 2024
Revised: August 14, 2024
Accepted: August 14, 2024
Published: August 19, 2024

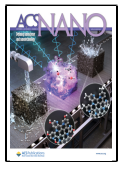

https://doi.org/10.1021/acsnano.4c08776
ACS Nano 2024, 18, 24523−24531

the neutral exciton emission, whereas the origin of the other lines is still under debate. Possible explanations that have been given are phonon modes,[23] higher excitonic states,[26,27] excimers,[28] free excitons,[29] or biexcitons.[30] Recently, several publications provided strong arguments to attribute the low energy line of the multiplet to a negative trion emission.[25,31,32] A work that observed three peaks in one spectrum is published by Antolinez et al.[32] Here, the energetically highest line is attributed to an exciton transition, the middle one to the trion and the lowest energy line to an electron shakeup line of the trion, as detailed by the same group.[33] In contrast to the excitonic ground state, the trionic ground state is a spin singlet state that does not exhibit exchange splitting,[34] which leads to one major advantage compared to the excitonic one: with no dark/bright state splitting, trion emission is a favorable characteristic for single photon emitters that are used in quantum information applications. Therefore, developing a comprehensive understanding of the recombination mechanisms in NPLs, in particular the role of trion formation, its radiative emission, and methods to control it are critical for future applications.

In this work, we investigated 4 monolayer (ML) thick undoped and Cu-doped CdSe core NPLs by a plethora of optical spectroscopy techniques. Comparing ensemble measurements to single particle spectroscopy of undoped NPLs, we demonstrate how Förster resonant energy transfer (FRET) and hole trap states in stacks of NPLs induce enhanced trion emission, while single NPLs spectra are dominated by neutral excitonic emission. Time resolved photoluminescence spectroscopy of NPL films with different layer thickness is used to understand the dynamics of trion formation and p-state emission, respectively. We confirm trap assisted trion formation by adjusting the thickness of a NPL film and intentional copper doping, respectively, paving the path for deliberately tuning trion formation and emission.

Sample preparation including the synthesis of 4 ML CdSe NPLs (thickness: ∼1.2 nm)[35] and in situ Cu-doped CdSe NPLs are detailed in the method section and can be found elsewhere.[13,15,30,36,37] To identify the dominant emission lines of the NPLs, we compared temperature-dependent emission and absorption spectra of drop casted thick films (Figure 1). The absorption is dominated over the entire temperature range by a low energetic heavy hole exciton transition (∼2.45 eV at 290 K) and a high energetic light hole exciton transition (∼2.6 eV at 290 K) as expected.[4,38,39] The PL, however, shows at 50 K two clearly distinguishable emission lines that are energetically below the absorption resonance of the heavy hole exciton. With rising temperature, the low energy emission line apparently vanishes. As the absorption resonance of the heavy hole exciton clearly follows the high energy emission line, we conclude that the high energy line of the emission doublet is of neutral excitonic origin (X^0). Obviously, the low energy line of the doublet does not originate from electronically coupled quantum wells in the NPL stacks as an electronic coupling would also imply a shift in the absorption spectra. Thus, the low energy line of the doublet can be attributed to trion emission (X^-), in agreement with literature.[25,31,32]

The detailed normalized temperature-dependent macro-PL spectra of a drop cast film of 4 ML thick, undoped CdSe NPLs are shown in Figure 2a. With increasing temperature, the ratio between trion and exciton emission decreases continuously, which is explained by thermally activated nonradiative Auger recombination that directly competes with radiative trion emission.[32] A detailed explanation of the competing recombination mechanisms in this material system is given below.

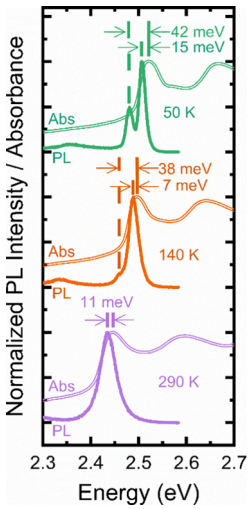

Figure 1. Comparison of the temperature-dependent absorbance (Abs) and photoluminescence (PL) spectra of 4 ML thick CdSe NPLs. Indicated energy values mark the Stokes shift of the emission lines with respect to the heavy hole absorption peak.

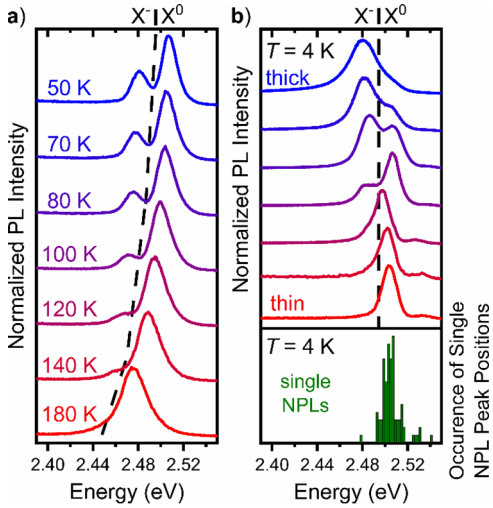

Figure 2. a) Temperature-dependent normalized PL spectra of 4 ML thick CdSe NPLs. Dashed line is a guide to the eye emphasizing the center between the neutral exciton (X^0) and the trion emission line (X^-) with rising temperature. b) Top: Film thickness dependent normalized PL spectra of the same batch of 4 ML CdSe NPLs at T = 4 K for film thicknesses of ∼350 to ∼10 nm (topography details are provided in Figure SI1). Dashed line is a guide to the eye to distinguish between the neutral exciton and the trion emission. Bottom: histogram of the occurrence of the emission peak positions of 90 single NPL spectra at T = 4 K.

The film thickness dependent micro-PL spectra of the same batch of NPLs are depicted in Figure 2b (top). The total thickness in the figure ranges from ∼350 to ∼10 nm as confirmed by confocal optical microscopy (Figure SI1). Interestingly, the film thickness has a strong influence on the PL signatures: The larger the film thickness, the more dominant the trion emission in comparison to the exciton one. This raises the question, whether collective effects caused by stacking the NPLs are boosting trion emission. It must be noted that in addition to the two main emission lines, a third

https://doi.org/10.1021/acsnano.4c08776
ACS Nano 2024, 18, 24523−24531

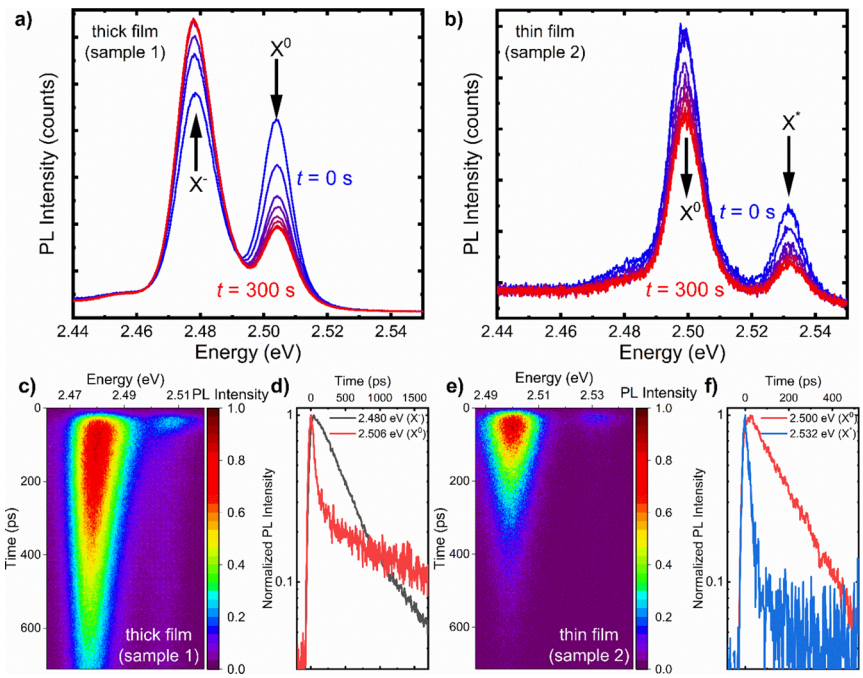

Figure 3. PL spectra of (a) a drop casted thick film (sample 1) and (b) a diluted and spin coated thin film (sample 2) of the same batch of 4 ML thick CdSe NPLs at 7 K, measured under the same conditions. Peaks are named as X^- (trion), X^0 (exciton), and X* (higher excitonic state). Measurements have been performed between 0 s (blue) and 300 s (red) of laser illumination with an integration time of 0.5 s per spectrum (a, thick film) and 1 s per spectrum (b, thin film), respectively. (c) Color plots of TRPL spectra at 7 K of the thick film (X^- and X^0 are visible) and (e) of the thin film (X^0 and X* are visible), respectively. (d, f) Corresponding decay curves extracted from the data shown in (c, e), respectively, averaged over ±1 meV around the given energy.

emission feature appears at the higher energy side of the spectrum at approximately 2.53 eV for smaller film thicknesses (Figure 2b), which will be discussed in more detail below.

To completely prevent interactions between NPLs and their stacking, single NPL spectroscopy is a powerful tool (detailed sample preparation in SI). A histogram of the peak positions collected from 90 different single NPL spectra is shown in Figure 2b (bottom, see Figure SI2 for some exemplary spectra). Interestingly, the single NPL spectra are clearly dominated by neutral excitonic emission with negligible trionic emission.

Since we expect the energetical lowest emission line to originate from a trion, we aim to test for trionic behavior. One strong indication of trion emission is photo charging via laser illumination that is expected to lead to an enhancement of the trion emission compared to the excitonic one due to hole trapping, e.g., by surface defect states.[31] We compare photo charging in thick NPL film (thickness ∼350 nm, sample 1) having a large amount of NPL stacks with a thin film (thickness ∼10 nm, sample 2) with negligible stacking, and measured them under the exact same conditions (see SI for preparation and experimental details). Confocal microscopy topography measurements have been used to extract the respective film thickness (Figure SI1).

The change of the PL emission during 300 s of laser illumination at T = 7 K is presented in Figure 3a (thick film, sample 1) and Figure 3b (thin film, sample 2). For a better understanding, the three main peaks that can be observed in these two samples are named according to our assignment. The trion X^- is the low energy line and the neutral exciton X^0 is the medium one, whereas the high energy line is named X*. Note that X* is not observed in the thick film and X^- is neglectable in the thin film.

In the case of the thick film, photo darkening for the exciton is observed, while at the same time, the trion emission is getting stronger. This is indeed in accordance with the expected behavior for those two lines and supports the assignment of the X^0 and X^- lines as outlined above and discussed in ref 31. The behavior for the thin sample differs significantly from that of the thick one. Here, photo darkening is observed for both, X^0 and X* emission, which strongly suggests that none of the two main peaks in Figure 3b originates from a trion emission. Thus, they might have an excitonic origin. The origin of X* could potentially be related to excitons formed from the *p*-states of electrons and holes, respectively, as it was argued by Achtstein et al.[26] Another argument against trion formation in the thin film is the different energy spacing between X^- and X^0 (26 meV, Figure 3a) and X^0 and X* (32 meV, Figure 3b). We can safely conclude that the exciton (X^0) is always visible, while the trion (X^-) is only visible in thick films, and the emission from a higher energetic state (X*) is only visible in thin films.

The tentative assignments of the three peaks need further proof. Each recombination mechanism follows a specific radiative decay rate, which can be accessed by time-resolved fluorescence (TRPL) spectroscopy. For that purpose, we performed TRPL spectroscopy on the exact same samples discussed in Figure 3a,b directly after the photo charging experiments. Streak camera images of the emission from thick and thin films are depicted in Figure 3c,e, respectively. Figure 3c shows the PL traces of X^- (lower energy, longer decay time) and X^0 (higher energy, shorter decay time) emission, whereas Figure 3e visualizes the PL traces of X^0 (lower energy, longer decay time) and X* (higher energy, shorter decay time) emission. Selected PL spectra at specific times are shown in

https://doi.org/10.1021/acsnano.4c08776
ACS Nano 2024, 18, 24523−24531

Figure SI3. Associated normalized PL decay curves for specific energies are depicted in Figure 3d,f, respectively.

Based on the photo charging studies of the thin film (Figure 3b), we assigned the X* line to neutral *p*-like higher excitonic states, in accordance with literature.[27,40] After excitation, a fast relaxation from these *p*-states into the ground *s*-states via phonon-assisted scattering is expected.[26] Indeed, the X* PL decay in Figure 3f) is dominated by a short time constant ($\tau \approx$ 21 ps). In addition, there is an offset of 26 ps between the PL maxima of X^0 and X* emission, which fits well with the lifetime of the short component of the X* line. Both hints to a very fast transfer from the higher excitonic *p*-states to the excitonic ground *s*-states. Ayari et al. solved the rate equations for the specific case of an upper *p*-state and a lower *s*-state and their results fit nicely to our TRPL data of the thin film.[41] In the work of Achtstein et al.[26] it is claimed that the splitting between ground and excited states depends on the lateral NPL sizes. In our case the energy splitting is 32 meV, which would lead to an NPL area of approximately 175 nm^2, which is in good agreement with our NPL sizes of (15.3 ± 0.9) x (13.7 ± 1.6) nm^2 as confirmed by TEM images (Figure SI4).

The radiative trion lifetime is expected to be in the range of several 100 ps.[31] Indeed, for the thick film, the trion (X^-) decays approximately monoexponentially in the observed time frame with a lifetime $\tau \approx$ 450 ps (Figure 3d, black curve). In contrast, the neutral exciton (X^0) decay consists of a short component ($\tau_1 \approx$ 55 ps) and a long one ($\tau_2 \approx$ 800 ps) (see Figure 3d, red curve). These two components are often attributed to a fast relaxation of the exciton from the bright into the dark state (bright dark splitting ∼5 meV for 4 ML CdSe NPLs),[24,25] followed by the slow recombination from the dark state that leads to the long component if the temperature is below 10 K.[25,31,42] In our case, however, the X^0 emission in the thin film (Figure 3f, red curve) decays monoexponentially with a lifetime of $\tau \approx$ 140 ps. This apparently contradicts to the interpretation that the biexponential decay of the neutral exciton X^0 seen in the thick film (Figure 3d) is related to the interplay between bright and dark exciton emission.

Interestingly, in the thick film, the neutral exciton X^0 decays directly after excitation, whereas there is an offset of ∼80 ps until the trion emission X^- reaches its maximum. I.e. at time zero there is no trion formed yet, but formation takes some time. We thus attribute the fast decay component of the neutral exciton decay (Figure 3d) to trion formation, i.e. trions form out of neutral excitons in thick NPL layers. In contrast, trion formation is inhibited in thin NPL layers.

These results show unambiguously a strong influence of the film thickness and thus of the coupling between the NPLs on the photoluminescence, particularly the trion emission. To fathom how a thick film can lead to enhanced trion emission, it is necessary to understand that NPLs tend to self-assemble into stacks if the conditions are appropriate. For the thick films formed by drop casting, the amount of NPLs on the substrate is much higher and the time to form a superstructure is very long, which leads to a stacking of the NPLs (see Figure SI4, NPLs have been drop casted onto a TEM grid). By spin coating the NPL onto the substrate as done for the thin film, the NPLs are driven apart from each other and tend to be more isolated. Thus, we suppose that the main difference between a "thick film" and a "thin film" is the varying ratio of stacked and individual NPLs and the height of NPL stacks.

Importantly, in a stack of NPLs an additional ultrafast mechanism of Förster resonant energy transfer (FRET) needs to be considered,[18] which leads to an ultraefficient exciton transfer between the stacked NPLs and is not present in isolated NPLs. The transfer happens nonradiatively via dipole−dipole exchange interactions. It has been shown that the heavy-hole exciton transition dipoles in NPLs are strongly in-plane oriented. This results in a directed out-of-plane emission that favors the efficiency of the transfer.[43] For an efficient FRET, a spectral overlap of the absorption spectrum of the transferring donor material and the emission spectrum of the receiving acceptor material is necessary. Due to the low Stokes shift, CdSe NPLs fulfill this condition excellently. It has been shown that exciton migration via homo-FRET (i.e., FRET between the same species) like in our case can be over a range of more than 100 nm with an exciton transfer time of 3 ps.[20] Moreover it is important to know that CdSe NPLs are prone to have defect states due to poor surface passivation[44−46] or Cd vacancies,[47−49] that can efficiently trap the holes.[20,50]

Taking the above-mentioned effects into account, the enhanced trion emission in thick films, i.e., stacked NPLs, can be explained. The proposed model is shown in Figure 4. Assuming an exciton generation in a NPL inside a stack, the fastest mechanism that is present in the system is homo-FRET. A NPL with defect states can trap the hole of the migrating exciton efficiently.[51] The more extended the NPL stack the more likely a hole is getting trapped, and the electron stays in the same NPL as the only free charge carrier, since FRET is now suppressed. If now a second exciton is generated somewhere in the NPL stack, it can get transferred through the stack via FRET and might at some point reach the NPL with the trapped hole and the free electron. In that case, a three-particle state forms, consisting of two electrons and one hole. This trion is pinned to that specific NPL by the trion binding energy and an efficient FRET to a neighboring platelet is less likely due to the enhanced Stokes shift of trion emission and exciton absorption. This three-particle state can now either recombine nonradiatively via Auger recombination or radiatively as a trion. Hole trapping and formation of a three-particle state has already been shown to quench exciton PL at room temperature, since the Auger pathway is faster than the radiative trion pathway under those conditions.[20,22] Since it has been shown experimentally in isolated NPL stacks that the FRET range can be as high as 500 nm,[19] we expect trion formation to increase the more NPLs are present within a stack, if the stack is smaller than the FRET range of about 500 nm.

With this model idea, we can now explain the origin of the three different emission lines as shown in Figures 2 and 3. The enhanced trion emission in stacked NPLs at low temperatures is due to the higher probability that a hole gets trapped in a distinct NPL of a stack and that a second exciton is excited in the same stack. As depicted in Figure 4, the second exciton can then be transferred to the NPL with the trapped hole and combine radiatively as a trion. This scenario can also explain the transient decay of exciton luminescence observed in drop-casted "thick" films, in which the short component of the exciton emission represents the dynamics of trion formation via FRET of a photogenerated exciton to a NPL with a trapped hole (Figure 3d). This fast component is not present for neutral exciton emission X^0 in the isolated NPL (see Figure 3f), since without FRET trion formation is less likely. Thus, the decay of the neutral exciton emission in "thin" films is due to radiative recombination, probably overlaid by some transfer of

https://doi.org/10.1021/acsnano.4c08776
ACS Nano 2024, 18, 24523−24531

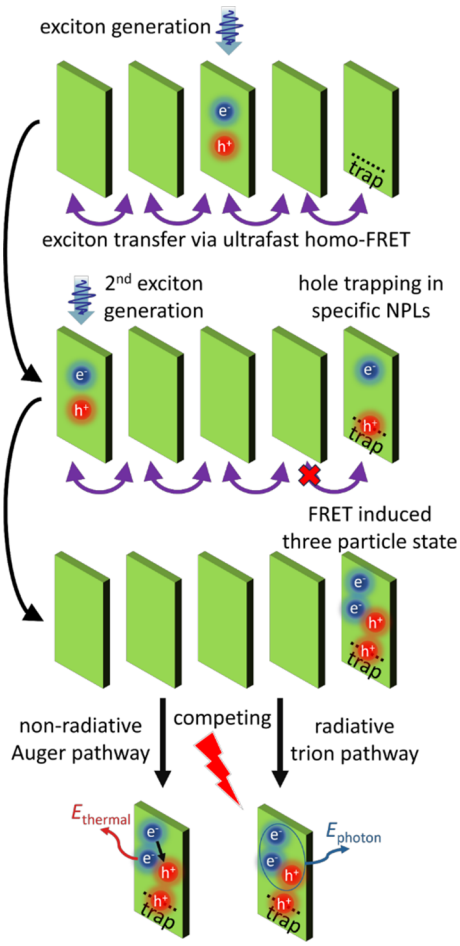

Figure 4. Model for a FRET-induced trion emission in a stack of self-assembled NPLs. Photogenerated electron−hole pair can funnel through the stack via ultrafast homo-FRET. Specific NPLs exhibit intra gap states that trap holes, leaving an electron behind. If a second exciton is excited in the same stack and reaches that NPL, a negatively charged trion arises (two electrons and one hole). Two pathways are possible at that point: nonradiative Auger and radiative trion recombination. Probability of both pathways depends on their respective recombination times, that can be changed by external parameters (e.g., temperature).

the bright exciton into the dark state. The reason why the *p*-state is only visible for isolated NPLs (see Figure 3b) might very well be that FRET is more efficient for higher excitonic states, which decreases the probability of a radiative emission of a p-state. This is caused by the larger overlap of CdSe absorption and p-state emission, which favors FRET.

The vanishing of the trion emission at elevated temperatures as seen in Figure 2a originates in a changing ratio of the lifetimes of the two pathways (radiative trion or nonradiative Auger recombination). First, the trion recombination rate at 5 K is significantly faster than at room temperature,[52,53] which makes the radiative path at low temperatures more likely. Second, the Auger recombination rate can increase with rising temperature. This is *e.g.* shown in core/shell quantum dots, where the thermal energy can delocalize one of the electrons of the trion to the surface leading to surface-assisted Auger recombination.[54] Additionally, an increase of the temperature can lead to a thermal detrapping of the captured hole, which can then lead to the formation of a biexciton complex that consists of four particles and possesses an Auger recombination rate approximately double the one from a trion.[55]

In the light of our findings, we may recap the emission characteristics of CdSe NPLs reported in literature. Achtstein et al.[26] embedded the NPLs in a polymer matrix to avoid any aggregation or FRET effects and found a distinct *p*-state luminescence like it is the case for our thin film samples (Figure 3b), where aggregation is suppressed. Shornikova et al.,[31] however, drop-casted the NPLs onto a substrate and observed prominent trion emission. Self-assembled NPL stacks can form as a result of the drop casting, and FRET can take place, which supports trion emission, in agreement with our results.

If hole trap states are responsible for the enhanced trion emission, it should be possible to intentionally dope the NPLs with a hole trapping element like copper, which is incorporated as Cu^+, to enhance trion emission. In the investigated sample the average number of copper dopants is about 200 (i.e., Cu/Cd atomic concentration of ∼1.2%) according to ref 37, where the same synthesis recipe was used. This dopant concentration ensures that hole trapping by Cu^+ states is the dominant mechanism compared to hole trapping by defects, while at the same time prevents Cu−Cu interactions. In Figure 5a) the

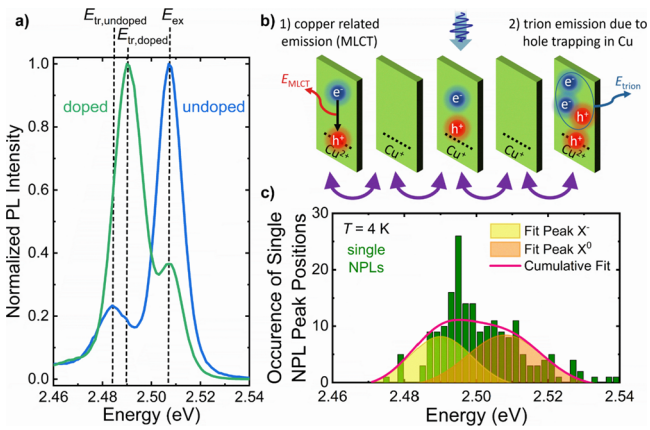

Figure 5. (a) Comparison of the macro PL spectra of an undoped (blue) and a copper doped (green) 4 ML CdSe NPL thick film at T = 10 K that were prepared with the same preparation route. Trion emission is enhanced upon doping. Peak position of the exciton (E_{ex}) is the same for both samples, whereas the trion binding energy for the doped sample ($E_{tr,doped}$) is smaller than for the undoped one ($E_{tr,undoped}$). (b) Extension of the model of Figure 4: copper states can serve as intentional hole traps to enhance the probability of a three-particle state. (c) Histogram of 199 evaluated single-particle doped NPL spectra at T = 4 K and the occurrence of their respective peak positions (dark green). Red line depicts the cumulative fit of the histogram with two Gaussian functions with given center energy of 2.49 eV for the trion (X^-, yellow) and of 2.508 eV for the exciton (X^0, orange) peak, respectively.

band edge PL at 10 K of a thick film of undoped 4 ML CdSe NPLs (data from Figure 2a) is compared to that of a 4 ML Cu:CdSe NPL film, that has been prepared in exactly the same way. An extended energy range of the PL spectra showing the copper transition is depicted in Figure SI5. Interestingly, the trion to exciton ratio is significantly enhanced in the doped sample, as expected by our model idea. The adapted model for copper doped systems is shown in Figure 5b). In contrast to undoped NPLs, in which not all NPLs have hole trap states,

https://doi.org/10.1021/acsnano.4c08776
ACS Nano 2024, 18, 24523−24531

now every NPL contains Cu^+ states close to the valence band. Thus, each NPL can trap a hole to change the oxidation state to Cu^{2+}, which drastically increases the probability of trapping holes. This trapped hole can now either recombine via metal to ligand charge transfer (MLCT) with the conduction band (CB) electron, which leads to the characteristic broad red emission of copper dopants (see Figure SI5). Alternatively, a second exciton is generated in the same stack of NPLs before recombination via copper states occurs, resulting in a trion and a trapped hole.

In a stack of undoped NPLs, two conditions need to be fulfilled for observing trion emission: (i) the first excited exciton needs to be transferred to a NPL with a trap via FRET and (ii) a second exciton needs to be excited in the same stack as long as the first hole is trapped. In a stack of doped NPLs, condition (i) is always fulfilled since in our samples the average number of Cu^+ ions per NPL exceeds 1 by far as mentioned above. Accordingly, hole traps exist for all NPLs and due to the long lifetime of the copper state (~2.7 μs at 17 K)[13] compared to other radiative channels at cryogenic temperatures, there is a high probability that a second exciton is generated in the same stack before MLCT recombination takes place. Thus, trion emission gets more likely. A further proof for the model is that the ratio between trion emission and copper emission is strongly power dependent even at low power densities, although copper states should not saturate in this specific case (see Figure SI5). For small excitation power densities, recombination via MLCT is more likely to happen before a second exciton reaches the trapped hole, whereas at high excitation power densities, the second exciton reaches the trapped hole before MLCT can happen and the trion intensity rises. A similar enhancement of the trion emission has already been reported for chemically doped CdSe NPLs with electron donors.[56,57]

Due to the high amount of hole trap states in Cu:CdSe NPLs, we expect an enhanced trion emission even for single NPLs since FRET is not necessary to reach a trap state. For that purpose, we evaluated the PL spectra of 199 different copper doped single NPLs (see Figure SI6 for exemplary spectra). The results are shown in Figure 5c in a histogram that can be compared to that of the undoped NPLs in Figure 2b (bottom). To elaborate the effect of trion emission, we fitted the data of the histogram with two Gaussian functions with fixed center energy derived from the ensemble spectrum in Figure 5a (X^-: 2.49 eV, X^0: 2.508 eV). The resulting cumulative fit is depicted with a red line and represents the data very nicely. This lets us conclude that the histogram derived from the single NPL spectra cannot be described by neutral excitonic emission only, but trion emission significantly contributes to the single particle spectra of Cu^+-doped CdSe NPLs, confirming our model idea. Interestingly, the proof of enhanced trion emission in single Cu-doped NPLs due to hole trapping is a strong indicator that Cu is indeed incorporated as Cu^+ into the CdSe lattice.

In summary, we identified three different low temperature emission pathways in 4 ML CdSe NPLs that are strongly dependent on the amount of NPL stacks in the observed system. Trion luminescence is shown to distinctively depend on the amount of hole traps in the system that are accessible by FRET, leading to enhanced trion formation if stacks of NPLs are present. In contrast, isolated NPL show dominantly neutral exciton emission. This model idea is confirmed by implementing copper into CdSe NPLs for creating intentional hole traps, leading to enhanced trion formation. Our results can thus consistently explain the controversial findings in literature for the low temperature NPL emission spectra.

METHODS

Materials. Sodium myristate (≥99.0%), cadmium nitrate tetrahydrate (≥99.0%), trioctylphosphine (TOP, 90%), copper(II) acetate, cadmium acetate dihydrate ($Cd(OAc)_2 \times 2H_2O$, 98%), selenium (99.99%), oleic acid (OA, 90%), 1-octadecene (ODE, 90%), *n*-hexane (≥97.0% and ≥99.0%), methanol (≥99.7%) and ethanol (absolute) were purchased from Sigma-Aldrich.

Synthesis of 4 ML CdSe Core NPLs. Four ML CdSe core NPLs were synthesized according to the recipe in the literature with minor modifications.[58] Beforehand, cadmium myristate was prepared according to a detailed recipe in the literature.[58] In a typical synthesis of CdSe core NPLs, 360 mg of cadmium myristate, 24 mg of Se and 30 mL of ODE were mixed in a 100 mL flask. The solution was degassed at 95 °C for 1 h and then the flask was flushed with the argon gas and the temperature was set to 238 °C. At a temperature between 190 and 195 °C, when the solution color turns into golden yellow, 190 mg of $Cd(OAc)_2 \times 2H_2O$ was swiftly added to the solution. The flask was kept at 238 °C for 6 min for a complete lateral growth of the NPLs and then 1 mL of OA was injected into the solution while the flask was quenched in a water bath. The solution was diluted with 8 mL of hexane and centrifuged at 6000 rpm for 6 min to precipitate out the heavy unwanted species. To precipitate the NPLs, extra amount of ethanol was added to the supernatant and the solution was centrifuged at 6000 rpm for 6 min. Finally, the precipitated NPLs were redispersed in 2 mL of hexane and kept for further use.

Synthesis of 4 ML Cu:CdSe NPLs. Cu:CdSe NPLs were synthesized following an in situ synthesis protocol similar to the CdSe core NPLs.[15] First, copper precursor was prepared by dissolving 7.5 mg of copper(II) acetate in 2.5 mL of ODE and 1 mL of TOP. The solution was mixed for an overnight in the glovebox. The synthesis procedure for Cu:CdSe NPLs is largely similar to the CdSe core NPLs, except that before the addition of of $Cd(OAc)_2 \times 2H_2O$, 150 μL of the Cu precursor was added slowly to the solution. The rest of the synthesis procedure was the same as CdSe core NPLs.

Preparation of NPL Films. Samples for the macro-PL spectra (Figures 1, 2a and 5a) and the micro-PL spectra of the thick film (Figure 3a) were prepared by drop casting 50 μL undiluted source dispersion (dispersant: *n*-hexane) onto a 300 nm SiO_2/Si substrate. Confocal microscopy information (e.g., thickness, homogeneity, and schematics of the whole sample) can be found in Figure SI1a,b. Samples for the micro-PL spectra of the thin film (four thinnest spots in Figures 2b and 3b) were prepared by diluting the source dispersion by a factor of 10 and spin coating 40 μL diluted dispersion onto a 300 nm SiO_2/Si substrate (see Table SI1 for detailed parameters). Confocal microscopy information (e.g., thickness, homogeneity, and schematics of the whole sample) about the thin film can be found in Figure SI1c,d.

To achieve a local variation of the film thickness (three thickest spots in Figure 2b), an additional drop of that diluted dispersion was placed onto the 300 nm SiO_2/Si substrate like shown in Figure SI1e–h. For that purpose, the pipet tip was dipped into the diluted dispersion and cautiously brought in contact with the sample. This leads to a droplet with decreasing thickness from center to edge.

Both samples shown in Figure 3 (sample 1, not diluted, 50 μL drop casted, see Figure 3a,c,d and sample 2, diluted by a factor of 10, 40 μL spin coated, see Figure 3b,e,f) were prepared and measured at the same day with the same batch of NPLs. The spin coating (sample 2) forces the NPLs to the outside of the substrate and leads to a uniform thin film (center ~10 nm, corner ~100 nm), whereas the drop casting (sample 1) lets the NPLs assemble themselves and leads to a thick film (center ~350 nm, corner ~300 nm). Further process steps like mounting in the cryostat and performing TIPL and TRPL experiments were also performed equally at the same setup and at the same day.

https://doi.org/10.1021/acsnano.4c08776
ACS Nano 2024, 18, 24523–24531

Single particle samples (Figures 2b and 5c) were prepared by diluting the source dispersion by a factor of 1000−10,000 without adding any polymers and spin coating them onto a 300 nm SiO_2/Si substrate (Table SI1).

Absorption Spectroscopy (Figure 1). For optical absorption measurements, an UV2550 ultraviolet−visible spectrophotometer from Shimadzu was used. For that purpose, NPLs have been drop casted onto quartz substrates. Temperature adjustment between 10 and 300 K was achieved by using a JANIS ST-500 cryostat.

Transmission Electron Microscopy (TEM, Figure SI4). TEM images were obtained using Tecnai G2 F30 microscope. The samples were prepared by drop-casting a 100x dilute NPLs solution on the copper grid.

Macro-PL Spectroscopy (Figures 1, 2a, and5a). Macro-PL spectra were recorded with a fluorescence spectrophotometer Fluorolog-3 (FL3−22) with a Picosecond Photon Detection Module (PPD 850) by Horiba Scientific with a xenon lamp operating at 450 nm as excitation source. Temperature adjustment between 10 and 300 K was achieved by using a JANIS ST-500 cryostat. Excitation and detection are simultaneously performed across the whole length of the substrate (power density: 400 $\mu W/cm^2$).

Micro-PL Spectroscopy (Figures 2b, 5c, SI2, SI5, and SI6). Photoluminescence spectra were recorded with a μ-PL spectroscopy setup consisting of a confocal microscope (Attocube attoCFM I, microscope LT-APO-Vis, NA: 0.82), inserted into a closed-cycle cryostat (minimum sample temperature: T = 4.0 K), which leads to a laser spot diameter of approximately 1 μm on the substrate. The sample chamber was filled with helium as an exchange gas to ensure the thermal coupling with the cooling environment. The excitation source was a 450 nm diode laser (PicoQuant LDH-D-C-450), that was combined with a cleanup filter (Thorlabs FBH450/10−25) and long-pass edge filter (Semrock - EdgeBasic BLP01−458R-25). Spectra were recorded using a liquid nitrogen-cooled charge-coupled device (CCD) camera (Horiba Symphony I, back-illuminated deep depletion 1-LS) in combination with a monochromator setup (Horiba Triax 550). This leads to a spectral resolution of 1.0 meV. Thickness dependent spectra in Figure 2b were recorded with a power density of 5.7 kW/cm^2 and single platelet spectra with varying excitation power densities ranging from 12 W/cm^2 to 5.7 kW/cm^2. The spectra were corrected for the spectral sensitivity of the setup.

(Time-Resolved) PL Spectroscopy (Figures 3 and SI3). PL spectroscopy was performed with a pulsed frequency doubled titanium-sapphire laser (Coherent Mira 900-D, frequency of 76 MHz, pulse width of 100 fs) with a laser wavelength of 405 nm (average power density: 450 W/cm^2). The time integrated (TI) PL spectra of the samples were collected with an iHR320 monochromator and a Symphony II CCD camera from HORIBA Scientific (spectral resolution: 1.3 meV). Time-resolved (TR) PL spectra were recorded under the same conditions with a Hamamatsu C5680 streak camera system operated in photon counting mode. For temperature adjustment, a Janis ST-300 cryostat cooled with liquid He was used.

ASSOCIATED CONTENT

Supporting Information

The Supporting Information is available free of charge at https://pubs.acs.org/doi/10.1021/acsnano.4c08776.

Additional experimental details, including NPL synthesis, sample preparation, setup details, TEM images of the used NPLs, optical images of thin and thick films, and additional optical spectroscopy data (PDF)

AUTHOR INFORMATION

Corresponding Author

Gerd Bacher − *Werkstoffe der Elektrotechnik and CENIDE, University of Duisburg-Essen, Duisburg 47057, Germany;* orcid.org/0000-0001-8419-2158; Email: gerd.bacher@uni-due.de

Authors

Maurizio Riesner − *Werkstoffe der Elektrotechnik and CENIDE, University of Duisburg-Essen, Duisburg 47057, Germany*

Farzan Shabani − *Department of Electrical and Electronics Engineering, Department of Physics, UNAM-Institute of Materials Science and Nanotechnology and National Nanotechnology Research Center, Bilkent University, Ankara 06800, Turkey;* orcid.org/0000-0003-2174-5960

Levin Zeylmans van Emmichoven − *Werkstoffe der Elektrotechnik and CENIDE, University of Duisburg-Essen, Duisburg 47057, Germany;* orcid.org/0009-0007-1193-3059

Julian Klein − *Werkstoffe der Elektrotechnik and CENIDE, University of Duisburg-Essen, Duisburg 47057, Germany;* orcid.org/0000-0003-2349-6953

Savas Delikanli − *Department of Electrical and Electronics Engineering, Department of Physics, UNAM-Institute of Materials Science and Nanotechnology and National Nanotechnology Research Center, Bilkent University, Ankara 06800, Turkey; LUMINOUS! Center of Excellence for Semiconductor Lighting and Displays, School of Electrical and Electronic Engineering, School of Physical and Materials Sciences, School of Materials Science and Nanotechnology, Nanyang Technological University, Singapore 639798, Singapore;* orcid.org/0000-0002-0613-8014

Rachel Fainblat − *Werkstoffe der Elektrotechnik and CENIDE, University of Duisburg-Essen, Duisburg 47057, Germany;* orcid.org/0000-0002-9488-2563

Hilmi Volkan Demir − *Department of Electrical and Electronics Engineering, Department of Physics, UNAM-Institute of Materials Science and Nanotechnology and National Nanotechnology Research Center, Bilkent University, Ankara 06800, Turkey; LUMINOUS! Center of Excellence for Semiconductor Lighting and Displays, School of Electrical and Electronic Engineering, School of Physical and Materials Sciences, School of Materials Science and Nanotechnology, Nanyang Technological University, Singapore 639798, Singapore;* orcid.org/0000-0003-1793-112X

Complete contact information is available at: https://pubs.acs.org/10.1021/acsnano.4c08776

Author Contributions

M.R., R.F., and G.B. conceived of the idea and designed the experiments. M.R. performed the TIPL, absorption and confocal microscopy measurements. F.S. performed NPLs synthesis and TEM measurements under the supervision of S.D. and H.V.D. L.Z.v.E. performed parts of the single platelet measurements and the power dependent PL spectroscopy. J.K. performed the TRPL measurements. M.R. and G.B. wrote the manuscript. All the authors contributed to finalizing the manuscript.

Funding

M.R., J.K., R.F., and G.B. were funded by the Deutsche Forschungsgemeinschaft (DFG, German Research Foundation) under Contract No. BA 1422/16 (project number: 399377107) and the German Israeli Project Cooperation (DIP) under Contract No. HE 3543/42−1. H.V.D. was funded by TUBITAK 20AG001, 121N395, and 121C266. H.V.D. also acknowledges the support from TUBA and

TUBITAK 2247-A National Leader Researchers Program (121C266).

Notes

The authors declare no competing financial interest.

ACKNOWLEDGMENTS

M.R., J.K., R.F., and G.B. acknowledge the Deutsche Forschungsgemeinschaft (DFG) under Contract No. BA 1422/16 (project number: 399377107) and the German Israeli Project Cooperation (DIP) under Contract No. HE 3543/42-1.

REFERENCES

(1) Ithurria, S.; Dubertret, B. Quasi 2D Colloidal CdSe Platelets with Thicknesses Controlled at the Atomic Level. *J. Am. Chem. Soc.* **2008**, *130*, 16504−16505.

(2) Nasilowski, M.; Mahler, B.; Lhuillier, E.; Ithurria, S.; Dubertret, B. Two-Dimensional Colloidal Nanocrystals. *Chem. Rev.* **2016**, *116*, 10934−10982.

(3) Chen, Z.; Nadal, B.; Mahler, B.; Aubin, H.; Dubertret, B. Quasi-2D Colloidal Semiconductor Nanoplatelets for Narrow Electroluminescence. *Adv. Funct. Mater.* **2014**, *24*, 295−302.

(4) Ithurria, S.; Tessier, M. D.; Mahler, B.; Lobo, R. P. S. M.; Dubertret, B.; Efros, A. L. Colloidal Nanoplatelets with Two-Dimensional Electronic Structure. *Nat. Mater.* **2011**, *10*, 936−941.

(5) Sharma, M.; Delikanli, S.; Demir, H. V. Two-Dimensional CdSe-Based Nanoplatelets: Their Heterostructures, Doping, Photophysical Properties, and Applications. *Proc. IEEE* **2020**, *108*, 655−675.

(6) Grim, J. Q.; Christodoulou, S.; Di Stasio, F.; Krahne, R.; Cingolani, R.; Manna, L.; Moreels, I. Continuous-Wave Biexciton Lasing at Room Temperature Using Solution-Processed Quantum Wells. *Nat. Nanotechnol.* **2014**, *9*, 891−895.

(7) Guzelturk, B.; Kelestemur, Y.; Olutas, M.; Delikanli, S.; Demir, H. V. Amplified Spontaneous Emission and Lasing in Colloidal Nanoplatelets. *ACS Nano* **2014**, *8*, 6599−6605.

(8) Liu, B.; Sharma, M.; Yu, J.; Shendre, S.; Hettiarachchi, C.; Sharma, A.; Yeltik, A.; Wang, L.; Sun, H.; Dang, C.; Demir, H. V. Light-Emitting Diodes with Cu-Doped Colloidal Quantum Wells: From Ultrapure Green Tunable Dual-Emission to White Light. *Small* **2019**, *15*, No. 1901983.

(9) Lee, J.; Yoo, K.; Liu, H.; Kang, J. Sensitivity Improvement of Hybrid Active Layer Containing 2D Nanoplatelets for Indirect X-Ray Detector. *Nanotechnology* **2022**, *33*, No. 405701.

(10) Lhuillier, E.; Dayen, J. F.; Thomas, D. O.; Robin, A.; Ithurria, S.; Aubin, H.; Dubertret, B. Phototransport in Colloidal Nanoplatelets Array. *Phys. Status Solidi C* **2016**, *13*, 526−529.

(11) Whitham, P. J.; Knowles, K. E.; Reid, P. J.; Gamelin, D. R. Photoluminescence Blinking and Reversible Electron Trapping in Copper-Doped CdSe Nanocrystals. *Nano Lett.* **2015**, *15*, 4045−4051.

(12) Knowles, K. E.; Hartstein, K. H.; Kilburn, T. B.; Marchioro, A.; Nelson, H. D.; Whitham, P. J.; Gamelin, D. R. Luminescent Colloidal Semiconductor Nanocrystals Containing Copper: Synthesis, Photophysics, and Applications. *Chem. Rev.* **2016**, *116*, 10820−10851.

(13) Sharma, M.; Olutas, M.; Yeltik, A.; Kelestemur, Y.; Sharma, A.; Delikanli, S.; Guzelturk, B.; Gungor, K.; McBride, J. R.; Demir, H. V. Understanding the Journey of Dopant Copper Ions in Atomically Flat Colloidal Nanocrystals of CdSe Nanoplatelets Using Partial Cation Exchange Reactions. *Chem. Mater.* **2018**, *30*, 3265−3275.

(14) Dufour, M.; Izquierdo, E.; Livache, C.; Martinez, B.; Silly, M. G.; Pons, T.; Lhuillier, E.; Delerue, C.; Ithurria, S. Doping as a Strategy to Tune Color of 2D Colloidal Nanoplatelets. *ACS Appl. Mater. Interfaces* **2019**, *11*, 10128−10134.

(15) Sharma, M.; Gungor, K.; Yeltik, A.; Olutas, M.; Guzelturk, B.; Kelestemur, Y.; Erdem, T.; Delikanli, S.; McBride, J. R.; Demir, H. V. Near-Unity Emitting Copper-Doped Colloidal Semiconductor Quantum Wells for Luminescent Solar Concentrators. *Adv. Mater.* **2017**, *29*, No. 1700821.

(16) Ebrahimi, E.; Irfan, M.; Shabani, F.; Kocak, Y.; Karakurt, B.; Erdem, E.; Demir, H. V.; Ozensoy, E. Core-Crown Quantum Nanoplatelets with Favorable Type-II Heterojunctions Boost Charge Separation and Photocatalytic NO Oxidation on TiO2. *ChemCatChem.* **2020**, *12*, 6329−6343.

(17) Jones, G. A.; Bradshaw, D. S. Resonance Energy Transfer: From Fundamental Theory to Recent Applications. *Front. Phys.* **2019**, *7*, No. 00100.

(18) Rowland, C. E.; Fedin, I.; Zhang, H.; Gray, S. K.; Govorov, A. O.; Talapin, D. V.; Schaller, R. D. Picosecond Energy Transfer and Multiexciton Transfer Outpaces Auger Recombination in Binary CdSe Nanoplatelet Solids. *Nat. Mater.* **2015**, *14*, 484−489.

(19) Liu, J.; Guillemeney, L.; Abécassis, B.; Coolen, L. Long Range Energy Transfer in Self-Assembled Stacks of Semiconducting Nanoplatelets. *Nano Lett.* **2020**, *20*, 3465−3470.

(20) Guzelturk, B.; Erdem, O.; Olutas, M.; Kelestemur, Y.; Demir, H. V. Stacking in Colloidal Nanoplatelets: Tuning Excitonic Properties. *ACS Nano* **2014**, *8*, 12524−12533.

(21) Ouzit, Z.; Baillard, G.; Liu, J.; Wagnon, B.; Guillemeney, L.; Abécassis, B.; Coolen, L. Luminescence Dynamics of Single Self-Assembled Chains of Förster (FRET)-Coupled CdSe Nanoplatelets. *J. Phys. Chem. Lett.* **2023**, *12*, 6209−6216.

(22) Ouzit, Z.; Liu, J.; Pintor, J.; Wagnon, B.; Guillemeney, L.; Abécassis, B.; Coolen, L. FRET-Mediated Collective Blinking of Self-Assembled Stacks of CdSe Semiconducting Nanoplatelets. *ACS Photonics* **2023**, *10*, 421−429.

(23) Tessier, M. D.; Biadala, L.; Bouet, C.; Ithurria, S.; Abecassis, B.; Dubertret, B. Phonon Line Emission Revealed by Self-Assembly of Colloidal Nanoplatelets. *ACS Nano* **2013**, *7*, 3332−3340.

(24) Biadala, L.; Liu, F.; Tessier, M. D.; Yakovlev, D. R.; Dubertret, B.; Bayer, M. Recombination Dynamics of Band Edge Excitons in Quasi-Two-Dimensional CdSe Nanoplatelets. *Nano Lett.* **2014**, *14*, 1134−1139.

(25) Shornikova, E. V.; Biadala, L.; Yakovlev, D. R.; Sapega, V. F.; Kusrayev, Y. G.; Mitioglu, A. A.; Ballottin, M. V.; Christianen, P. C. M.; Belykh, V. V.; Kochiev, M. V.; Sibeldin, N. N.; Golovatenko, A. A.; Rodina, A. V.; Gippius, N. A.; Kuntzmann, A.; Jiang, Y.; Nasilowski, M.; Dubertret, B.; Bayer, M. Addressing the Exciton Fine Structure in Colloidal Nanocrystals: The Case of CdSe Nanoplatelets. *Nanoscale* **2018**, *10*, 646−656.

(26) Achtstein, A. W.; Scott, R.; Kickhöfel, S.; Jagsch, S. T.; Christodoulou, S.; Bertrand, G. H. V.; Prudnikau, A. V.; Antanovich, A.; Artemyev, M.; Moreels, I.; Schliwa, A.; Woggon, U. P-State Luminescence in CdSe Nanoplatelets: Role of Lateral Confinement and a Longitudinal Optical Phonon Bottleneck. *Phys. Rev. Lett.* **2016**, *116*, No. 116802.

(27) Specht, J. F.; Scott, R.; Corona Castro, M.; Christodoulou, S.; Bertrand, G. H. V.; Prudnikau, A. V.; Antanovich, A.; Siebbeles, L. D. A.; Owschimikow, N.; Moreels, I.; Artemyev, M.; Woggon, U.; Achtstein, A. W.; Richter, M. Size-Dependent Exciton Substructure in CdSe Nanoplatelets and Its Relation to Photoluminescence Dynamics. *Nanoscale* **2019**, *11*, 12230−12241.

(28) Diroll, B. T.; Cho, W.; Coropceanu, I.; Harvey, S. M.; Brumberg, A.; Holtgrewe, N.; Crooker, S. A.; Wasielewski, M. R.; Prakapenka, V. B.; Talapin, D. V.; Schaller, R. D. Semiconductor Nanoplatelet Excimers. *Nano Lett.* **2018**, *18*, 6948−6953.

(29) Yu, J.; Zhang, C.; Pang, G.; Sun, X. W.; Chen, R. Effect of Lateral Size and Surface Passivation on the Near-Band-Edge Excitonic Emission from Quasi-Two-Dimensional CdSe Nanoplatelets. *ACS Appl. Mater. Interfaces* **2019**, *11*, 41821−41827.

(30) Yu, J.; Sharma, M.; Li, M.; Liu, B.; Hernández-Martínez, P. L.; Delikanli, S.; Sharma, A.; Altintas, Y.; Hettiarachchi, C.; Sum, T. C.; Demir, H. V.; Dang, C. Efficient Generation of Emissive Many-Body Correlations in Copper-Doped Colloidal Quantum Wells. *Cell Reports Phys. Sci.* **2022**, *3*, No. 101049.

(31) Shornikova, E. V.; Yakovlev, D. R.; Biadala, L.; Crooker, S. A.; Belykh, V. V.; Kochiev, M. V.; Kuntzmann, A.; Nasilowski, M.; Dubertret, B.; Bayer, M. Negatively Charged Excitons in CdSe Nanoplatelets. *Nano Lett.* **2020**, *20*, 1370−1377.

https://doi.org/10.1021/acsnano.4c08776
ACS Nano 2024, 18, 24523−24531

(32) Antolinez, F. V.; Rabouw, F. T.; Rossinelli, A. A.; Keitel, R. C.; Cocina, A.; Becker, M. A.; Norris, D. J. Trion Emission Dominates the Low-Temperature Photoluminescence of CdSe Nanoplatelets. *Nano Lett.* **2020**, *20*, 5814−5820.
(33) Antolinez, F. V.; Rabouw, F. T.; Rossinelli, A. A.; Cui, J.; Norris, D. J. Observation of Electron Shakeup in CdSe/CdS Core/Shell Nanoplatelets. *Nano Lett.* **2019**, *19*, 8495−8502.
(34) Califano, M.; Franceschetti, A.; Zunger, A. Lifetime and Polarization of the Radiative Decay of Excitons, Biexcitons, and Trions in CdSe Nanocrystal Quantum Dots. *Phys. Rev. B - Condens. Matter Mater. Phys.* **2007**, *75*, No. 115401.
(35) Olutas, M.; Guzelturk, B.; Kelestemur, Y.; Yeltik, A.; Delikanli, S.; Demir, H. V. Lateral Size-Dependent Spontaneous and Stimulated Emission Properties in Colloidal CdSe Nanoplatelets. *ACS Nano* **2015**, *9*, 5041−5050.
(36) Yu, J.; Sharma, M.; Li, M.; Delikanli, S.; Sharma, A.; Taimoor, M.; Altintas, Y.; McBride, J. R.; Kusserow, T.; Sum, T. C.; Demir, H. V.; Dang, C. Low-Threshold Lasing from Copper-Doped CdSe Colloidal Quantum Wells. *Laser Photonics Rev.* **2021**, *15*, No. 2100034.
(37) Yu, J.; Hu, S.; Gao, H.; Delikanli, S.; Liu, B.; Jasieniak, J. J.; Sharma, M.; Demir, H. V. Observation of Phonon Cascades in Cu-Doped Colloidal Quantum Wells. *Nano Lett.* **2022**, *22*, 10224−10231.
(38) Liu, Y. H.; Wayman, V. L.; Gibbons, P. C.; Loomis, R. A.; Buhro, W. E. Origin of High Photoluminescence Efficiencies in CdSe Quantum Belts. *Nano Lett.* **2010**, *10*, 352−357.
(39) Muckel, F.; Delikanli, S.; Hernández-Martínez, P. L.; Priesner, T.; Lorenz, S.; Ackermann, J.; Sharma, M.; Demir, H. V.; Bacher, G. Sp-d Exchange Interactions in Wave Function Engineered Colloidal CdSe/Mn:CdS Hetero-Nanoplatelets. *Nano Lett.* **2018**, *18*, 2047−2053.
(40) Richter, M. Nanoplatelets as Material System between Strong Confinement and Weak Confinement. *Phys. Rev. Mater.* **2017**, *1*, No. 016001.
(41) Ayari, S.; Quick, M. T.; Owschimikow, N.; Christodoulou, S.; Bertrand, G. H. V.; Artemyev, M.; Moreels, I.; Woggon, U.; Jaziri, S.; Achtstein, A. W. Tuning Trion Binding Energy and Oscillator Strength in a Laterally Finite 2D System: CdSe Nanoplatelets as a Model System for Trion Properties. *Nanoscale* **2020**, *12*, 14448−14458.
(42) Morgan, D. P.; Kelley, D. F. Exciton Localization and Radiative Lifetimes in CdSe Nanoplatelets. *J. Phys. Chem. C* **2019**, *123*, 18665−18675.
(43) Scott, R.; Heckmann, J.; Prudnikau, A. V.; Antanovich, A.; Mikhailov, A.; Owschimikow, N.; Artemyev, M.; Climente, J. I.; Woggon, U.; Grosse, N. B.; Achtstein, A. W. Directed Emission of CdSe Nanoplatelets Originating from Strongly Anisotropic 2D Electronic Structure. *Nat. Nanotechnol.* **2017**, *12*, 1155−1160.
(44) Califano, M.; Franceschetti, A.; Zunger, A. Temperature Dependence of Excitonic Radiative Decay in CdSe Quantum Dots: The Role of Surface Hole Traps. *Nano Lett.* **2005**, *5*, 2360−2364.
(45) Knowles, K. E.; McArthur, E. A.; Weiss, E. A. A Multi-Timescale Map of Radiative and Nonradiative Decay Pathways for Excitons in CdSe Quantum Dots. *ACS Nano* **2011**, *5*, 2026−2035.
(46) Gómez-Campos, F. M.; Califano, M. Hole Surface Trapping in CdSe Nanocrystals: Dynamics, Rate Fluctuations, and Implications for Blinking. *Nano Lett.* **2012**, *12*, 4508−4517.
(47) Vietmeyer, F.; Tchelidze, T.; Tsou, V.; Janko, B.; Kuno, M. Electric Field-Induced Emission Enhancement and Modulation in Individual CdSe Nanowires. *ACS Nano* **2012**, *6*, 9133−9140.
(48) Türe, I. E.; Poulin, F.; Brinkman, A. W.; Woods, J. Electron Traps and Deep Levels in Cadmium Selenide. *Phys. status solidi* **1983**, *77*, 535−544.
(49) Türe, I. E.; Claybourn, M.; Brinkman, A. W.; Woods, J. Defects in Cadmium Selenide. *J. Cryst. Growth* **1985**, *72*, 189−193.
(50) Kunneman, L. T.; Schins, J. M.; Pedetti, S.; Heuclin, H.; Grozema, F. C.; Houtepen, A. J.; Dubertret, B.; Siebbeles, L. D. A. Nature and Decay Pathways of Photoexcited States in CdSe and CdSe/CdS Nanoplatelets. *Nano Lett.* **2014**, *14*, 7039−7045.
(51) Achtstein, A. W.; Schliwa, A.; Prudnikau, A.; Hardzei, M.; Artemyev, M. V.; Thomsen, C.; Woggon, U. Electronic Structure and Exciton-Phonon Interaction in Two-Dimensional Colloidal CdSe Nanosheets. *Nano Lett.* **2012**, *12*, 3151−3157.
(52) Peng, L.; Otten, M.; Hazarika, A.; Coropceanu, I.; Cygorek, M.; Wiederrecht, G. P.; Hawrylak, P.; Talapin, D. V.; Ma, X. Bright Trion Emission from Semiconductor Nanoplatelets. *Phys. Rev. Mater.* **2020**, *4*, No. 056006.
(53) Brumberg, A.; Watkins, N. E.; Diroll, B. T.; Schaller, R. D. Acceleration of Biexciton Radiative Recombination at Low Temperature in CdSe Nanoplatelets. *Nano Lett.* **2022**, *22*, 6997−7004.
(54) Javaux, C.; Mahler, B.; Dubertret, B.; Shabaev, A.; Rodina, A. V.; Efros, A. L.; Yakovlev, D. R.; Liu, F.; Bayer, M.; Camps, G.; Biadala, L.; Buil, S.; Quelin, X.; Hermier, J. P. Thermal Activation of Non-Radiative Auger Recombination in Charged Colloidal Nanocrystals. *Nat. Nanotechnol.* **2013**, *8*, 206−212.
(55) Pelton, M.; Andrews, J. J.; Fedin, I.; Talapin, D. V.; Leng, H.; O'Leary, S. K. Nonmonotonic Dependence of Auger Recombination Rate on Shell Thickness for CdSe/CdS Core/Shell Nanoplatelets. *Nano Lett.* **2017**, *17*, 6900−6906.
(56) Vong, A. F.; Irgen-Gioro, S.; Wu, Y.; Weiss, E. A. Origin of Low Temperature Trion Emission in CdSe Nanoplatelets. *Nano Lett.* **2021**, *21*, 10040−10046.
(57) Wang, L.; Xiang, D.; Gao, K.; Wang, J.; Wu, K. Colloidal N-Doped CdSe and CdSe/ZnS Nanoplatelets. *J. Phys. Chem. Lett.* **2021**, *12*, 11259−11266.
(58) Shabani, F.; Martinez, P. L. H.; Shermet, N.; Korkut, H.; Sarpkaya, I.; Dehghanpour Baruj, H.; Delikanli, S.; Isik, F.; Durmusoglu, E. G.; Demir, H. V. Gradient Type-II CdSe/CdSeTe/CdTe Core/Crown/Crown Heteronanoplatelets with Asymmetric Shape and Disproportional Excitonic Properties. *Small* **2023**, *19*, No. 2205729.

https://doi.org/10.1021/acsnano.4c08776
ACS Nano 2024, 18, 24523−24531